します。本賞をご推薦いただきました産業医科大学医学部微生物学教室教授　谷口　初美先生に心より御礼申し上げます。また，長崎大学，大阪市立大学，国立感染症研究所，京都大学，浜松医科大学，九州大学，大阪大学，日本BCG製造株式会社，結核予防会結核研究所をはじめとする，多くのご支援いただいた先達の方々や研究仲間に，この場をかりて深く感謝申し上げます。

文　献

1) Aldovini, A., Young, R.A. (1991): Humoral and cell-mediated immune responses to live recombinant BCG-HIV vaccines [see comments]. Nature **351**, 479–482.
2) Ami, Y., Izumi, Y., Matsuo, K., Someya, K., Kanekiyo, M., Horibata, S., Yoshino, N., Sakai, K., Shinohara, K., Matsumoto, S., Yamada, T., Yamazaki, S., Yamamoto, N., Honda, M. (2005): Priming-boosting vaccination with recombinant *Mycobacterium bovis* bacillus Calmette-Guerin and a nonreplicating vaccinia virus recombinant leads to long-lasting and effective immunity. J. Virol. **79**, 12871–12879.
3) Aoki, K., Matsumoto, S., Hirayama, Y., Wada, T., Ozeki, Y., Niki, M., Domenech, P., Umemori, K., Yamamoto, S., Mineda, A., Matsumoto, M., Kobayashi, K. (2004): Extracellular mycobacterial DNA-binding Protein 1 participates in *Mycobacterium*-lung epithelial cell interaction through hyaluronic acid. J. Biol. Chem. **279**, 39798–39806.
4) Blackman, M.J., Heidrich, H.G., Donachie, S., McBride, J.S., Holder, A.A. (1990): A single fragment of a malaria merozoite surface protein remains on the parasite during red cell invasion and is the target of invasion-inhibiting antibodies. J. Exp. Med. **172**, 379–382.
5) Blackman, M.J., Scott, F.T., Shai, S., Holder, A.A. (1994): Antibodies inhibit the protease-mediated processing of a malaria merozoite surface protein. J. Exp. Med. **180**, 389–393.
6) Bloom, B.R. (2002): Tuberculosis—the global view. N. Engl. J. Med. **346**, 1434–1435.
7) Carrondo, M.A. (2003): Ferritins, iron uptake and storage from the bacterioferritin viewpoint. EMBO J. **22**, 1959–1968.
8) Chiancone, E., Ceci, P., Ilari, A., Ribacchi, F., Stefanini, S. (2004): Iron and proteins for iron storage and detoxification. Biometals **17**, 197–202.
9) Colangeli, R., Haq, A., Arcus, V.L., Summers, E., Magliozzo, R.S., McBride, A., Mitra, A.K., Radjainia, M., Khajo, A., Jacobs, W.R. Jr., Salgame, P., Alland, D. (2009): The multifunctional histone-like protein Lsr2 protects mycobacteria against reactive oxygen intermediates. Proc. Natl. Acad. Sci. USA **106**, 4414–4418.
10) Culty, M., Nguyen, H.A., Underhill, C.B. (1992): The hyaluronan receptor (CD44) participates in the uptake and degradation of hyaluronan. J. Cell. Biol. **116**, 1055–1062.
11) Ernst, J.D. (1998): Macrophage receptors for *Mycobacterium tuberculosis*. Infect. Immun. **66**, 1277–1281.
12) Forteza, R., Lieb, T., Aoki, T., Savani, R.C., Conner, G.E., Salathe, M. (2001): Hyaluronan serves a novel role in airway mucosal host defense. FASEB J. **15**, 2179–2186.
13) Furugen, M., Matsumoto, S., Matsuo, T., Matsumoto, M., Yamada, T. (2001): Identification of the mycobacterial DNA-binding protein 1 region which suppresses transcription in vitro. Microb. Pathog. **30**, 129–138.
14) Hershberg, R., Lipatov, M., Small, P.M., Sheffer, H., Niemann, S., Homolka, S., Roach, J.C., Kremer, K., Petrov, D.A., Feldman, M.W., Gagneux, S. (2008): High functional diversity in *Mycobacterium tuberculosis* driven by genetic drift and human demography. PLoS Biol. **6**, e311.
15) Hirayama, Y., Yoshimura, M., Ozeki, Y., Sugawara, I., Udagawa, T., Mizuno, S., Itano, N., Kimata, K., Tamaru, A., Ogura, H., Kobayashi, K., Matsumoto, S. (2009): Mycobacteria exploit host hyaluronan for efficient extracellular replication. PLoS Pathog. **5**, e1000643.
16) Katsube, T., Matsumoto, S., Takatsuka, M., Okuyama, M., Ozeki, Y., Naito, M., Nishiuchi, Y., Fujiwara, N., Yoshimura, M., Tsuboi, T., Torii, M., Oshitani, N., Arakawa, T., Kobayashi, K. (2007): Control of cell wall assembly by a histone-like protein in Mycobacteria. J. Bacteriol. **189**, 8241–8249.
17) Lewin, A., Baus, D., Kamal, E., Bon, F., Kunisch, R., Maurischat, S., Adonopoulou, M., Eich, K. (2008): The mycobacterial DNA-binding protein 1 (MDP1) from *Mycobacterium bovis* BCG influences various growth characteristics. BMC Microbiol. **8**, 91.
18) Matsumoto, S., Furugen, M., Yukitake, H., Yamada, T. (2000): The gene encoding mycobacterial DNA-binding protein 1 (MDP1) transformed rapidly growing bacteria to slowly growing bacteria. FEMS Microbiol. Lett. **182**, 297–301.
19) Matsumoto, S., Matsumoto, M., Umemori, K., Ozeki, Y., Furugen, M., Tatsuo, T., Hirayama, Y., Yamamoto, S., Yamada, T., Kobayashi, K. (2005): DNA augments antigenicity of mycobacterial DNA-binding protein 1 and confers protection against *Mycobacterium tuberculosis* infection in mice. J. Immunol. **175**, 441–449.
20) Matsumoto, S., Tamaki, M., Yukitake, H., Matsuo, T., Naito, M., Teraoka, H., Yamada, T. (1996): A stable *Escherichia coli*-mycobacteria shuttle vector 'pSO246' in *Mycobacterium bovis* BCG. FEMS Microbiol. Lett. **135**, 237–243.
21) Matsumoto, S., Yukitake, H., Furugen, M., Matsuo, T., Mineta, T., Yamada, T. (1999): Identification of a novel DNA-binding protein from *Mycobacterium bovis* bacillus Calmette-Guerin. Microbiol. Immunol. **43**, 1027–1036.
22) Matsumoto, S., Yukitake, H., Kanbara, H., Yamada, T. (1998): Recombinant *Mycobacterium bovis* bacillus Calmette-Guerin secreting merozoite surface protein 1 (MSP1) induces protection against rodent malaria parasite infection depending on MSP1-stimulated interferon gamma and parasite-specific antibodies. J. Exp. Med. **188**, 845–854.
23) Matsumoto, S., Yukitake, H., Kanbara, H., Yamada, T. (1999): Long-lasting protective immunity against rodent malaria parasite infection at the blood stage by recombinant BCG secreting merozoite surface protein-1. Vaccine **18**, 832–834.
24) Matsuo, K., Yamaguchi, R., Yamazaki, A., Tasaka, H., Terasaka, K., Yamada, T. (1990): Cloning and expression of the gene for the cross-reactive alpha antigen of Mycobacterium kansasii. Infect. Immun. **58**, 550–556.
25) Matsuo, K., Yamaguchi, R., Yamazaki, A., Tasaka, H., Terasaka, K., Totsuka, M., Kobayashi, K., Yukitake, H., Yamada, T. (1990): Establishment of a foreign antigen secretion system in mycobacteria. Infect. Immun. **58**, 4049–4054.
26) Matsuo, K., Yamaguchi, R., Yamazaki, A., Tasaka, H., Yamada, T. (1988): Cloning and expression of the *Mycobacterium bovis* BCG gene for extracellular alpha antigen. J. Bacteriol. **170**, 3847–3854.
27) Menozzi, F.D., Rouse, J.H., Alavi, M., Laude-Sharp, M., Muller, J., Bischoff, R., Brennan, M.J., Locht, C. (1996): Identification of a heparin-binding hemagglutinin present in mycobacteria. J. Exp. Med. **184**, 993–1001.
28) Rauzier, J., Moniz-Pereira, J., Gicquel-Sanzey, B. (1988):

Complete nucleotide sequence of pAL5000, a plasmid from *Mycobacterium fortuitum*. Gene **71**, 315–321.

29) Sassetti, C.M., Boyd, D.H., Rubin, E.J. (2003): Genes required for mycobacterial growth defined by high density mutagenesis. Mol. Microbiol. **48**, 77–84.

30) Stover, C.K., de la Cruz, V.F., Fuerst, T.R., Burlein, J.E., Benson, L.A., Bennett, L.T., Bansal, G.P., Young, J.F., Lee, M.H., Hatfull, G.F., *et al.* (1991): New use of BCG for recombinant vaccines. Nature **351**, 456–460.

31) Takatsuka, M., Osada-Oka, M., Satoh, E.F., Kitadokoro, K., Nishiuchi, Y., Niki, M., Inoue, M., Iwai, K., Arakawa, T., Shimoji, Y., Ogura, H., Kobayashi, K., Rambukkana, A., Matsumoto, S. (2011): A histone-like protein of Mycobacteria possesses ferritin superfamily protein-like activity and protects against DNA damage by Fenton reaction. PLoS One **6**, e20985.

32) Tolmasoff, J.M., Ono, T., Cutler, R.G. (1980): Superoxide dismutase: correlation with life-span and specific metabolic rate in primate species. Proc. Natl. Acad. Sci. USA **77**, 2777–2781.

33) Wayne, L.G., Sohaskey, C.D. (2001): Nonreplicating persistence of *Mycobacterium tuberculosis*. Annu. Rev. Microbiol. **55**, 139–163.

34) Wirth, T., Hildebrand, F., Allix-Beguec, C., Wolbeling, F., Kubica, T., Kremer, K., van Soolingen, D., Rusch-Gerdes, S., Locht, C., Brisse, S., Meyer, A., Supply, P., Niemann, S. (2008): Origin, spread and demography of the *Mycobacterium tuberculosis* complex. PLoS Pathog. **4**, e1000160.

35) Yamada, H., Matsumoto, S., Matsumoto, T., Yamada, T., Yamashita, U. (2000): Murine IL-2 secreting recombinant Bacillus Calmette-Guerin augments macrophage-mediated cytotoxicity against murine bladder cancer MBT-2. J. Urol. **164**, 526–531.

36) Yamamoto, S., Yamamoto, T., Kataoka, T., Kuramoto, E., Yano, O., Tokunaga, T. (1992): Unique palindromic sequences in synthetic oligonucleotides are required to induce IFN [correction of INF] and augment IFN-mediated [correction of INF] natural killer activity. J. Immunol. **148**, 4072–4076.

37) Yuan, Y., Crane, D.D., Barry, C.E. 3rd (1996): Stationary phase-associated protein expression in *Mycobacterium tuberculosis*: function of the mycobacterial alpha-crystallin homolog. J. Bacteriol. **178**, 4484–4492.

トピックス

結核研究の新たな展開
—潜在性結核と結核菌：休眠現象の分子メカニズム—

仁木 満美子[*1]　仁木　誠[*1]　尾関 百合子[*1*2]
岡 真優子[*1]　松本 壮吉[**1]

要　旨

結核は，年間 180 万人の命を奪う最大級の細菌感染症である．結核菌はヒトの寄生菌であり，中間宿主は存在しないことから，活動性結核に加え，病原体の源泉である潜在性結核の対処が疾患のコントロールに重要である．潜在期において結核菌は休眠しており，現行の薬剤に抵抗性である．休眠は，結核菌の長期間生存を保証する高次生命現象である．休眠のメカニズムを明らかにすることが，結核の抜本的対策に寄与すると考えられる．

はじめに

結核は，年間 180 万人の命を奪う最大級の細菌感染症である．結核の病原体は，グラム陽性細菌の結核菌（*Mycobacterium tuberculosis*）で，感染後も宿主の免疫に頑強に抵抗し，通常生体から排除されることはない．結核菌は有史前よりヒトに寄生し，ときに発症することで伝播してきた細菌であり，ヒトの寄生菌である．現在，推定で 1/3 の人類に感染している．潜在期において，多くの結核菌は増殖を停止しているが，死滅せず，生存することができる．これを休眠（dormant）と呼び，未発症の結核菌感染症は潜在性結核と定義される．ヒト型結核の住み処はヒトに限定されることから，筆者らは活動性結核（結核患者）に加え，潜在性結核に対処することが結核の制圧に繋がると考え，結核の潜在化にかかわる休眠現象を解析している．本稿では，結核の潜在化や菌の休眠現象についての研究の歴史と今後の展望について解説する．

結核菌の休眠（dormant）

結核菌の特徴の 1 つに，休眠現象がある．一般に，休眠状態の結核菌は活発な代謝活動を行わず，増殖することなく生命を維持しており，宿主体内においても潜伏し続け，一定の確率で再増殖して結核を発症する．このため無症候の潜伏感染を潜在性結核と呼んでいる．現在世界人口の 1/3 が結核菌に感染しており，一部は活動性結核（結核）で，ほとんどが潜在性結核である．また，全世界の結核死亡数は年間およそ 180 万人（2010 年，世界保健機構報告）に上るが，その多くが過去に感染し，休眠状態にあった結核菌の再燃によるものであるとされている．

結核菌は他の抗酸菌と異なり，環境や動物中で生育することができないことから，筆者らはヒト体内の休眠菌の駆逐が結核の制圧に繋がると考えている．現在の抗結核薬は休眠菌には効

[*1] 大阪市立大学大学院医学研究科 細菌学分野
[**1] 同 准教授
[*2] 園田学園女子大学人間健康学部 食物栄養学科 教授
キーワード：結核，休眠，潜在性結核，内因性再燃，LTBI

果に乏しく，結核治療には少なくとも6ヵ月を要するが，増殖菌と休眠菌の両方を殺傷する薬剤が開発できれば理論上2週間で結核治療が可能となる．

以上の事実と考察から，休眠状態の結核菌がいかにして増殖を停止した状態で生命を維持するかのメカニズムを解明することにより，新たな結核診断・治療法の開発の糸口が得られると考えられる．

実験的休眠モデル

では，実際に休眠菌とはどのように定義されるのか？菌がどのような生体環境下に置かれた場合に休眠状態に陥るかについては未解明のままであるものの，多くの科学者たちが *in vitro* における実験的休眠モデルを幾つか提案している．

結核菌を炭素源を除去した寒天培地に接種すると，結核病巣の組織切片で観察されるのと類似した形態および染色像を呈する菌体が得られるため，低栄養条件は実験的休眠モデルとして広く研究に活用されている．幾つかの研究により，低栄養状態の菌体は徐々に呼吸を最低限まで低下させるが死滅することはなく，栄養添加により増殖を再開させることや[1]，ストレス抵抗性の増加および mRNA の安定化，広範囲にわたるタンパク質合成の低下などを示すことが明らかになっている[2]．また遺伝子およびタンパク質発現解析によると，低栄養下の菌体はエネルギー代謝や脂質合成および細胞分裂を停止し[3]，環境に適応することで生命の維持を図っていると推察される．この実験方法は簡便かつ再現性を有するため，休眠菌の代謝研究に広く用いられている．

これに対し，肉芽腫内の休眠菌は酸素分圧の低い環境下にあると考えられることから[4]，低酸素を休眠誘導の方法として用いることも多い．Wayne らは，結核菌培養液から徐々に酸素を除去することで休眠を誘導する実験モデルを開発し[5]，菌の増殖停止期に2つのステージがあることを明らかにした[6]．

Wayne モデルの1つ目のステージ（nonreplicating persistence 1：NRP1）は溶存酸素濃度が1％まで減少した状態で，2つ目のステージ（nonreplicating persistence 2：NRP2）はそれがさらに 0.06% 未満にまで減少した状態のことを示す．NRP1 はいわゆる微好気状態であり，この段階における菌体は細胞壁の肥厚が見られ，生菌数および DNA 合成量が一定であるにもかかわらず，グリシンデヒドロゲナーゼ（GDH）の発現上昇および ATP 量の維持が認められる．これに対し NRP2 は嫌気状態に相当し，急激な GDH の減少が認められる．GDH の発現上昇は NRP1 後期における mRNA の合成を示唆しており，またこの酵素が，低酸素に菌が適応するために必要な NAD の再合成に関与すると考えられる．また NRP2 の菌体は，一般に潜在性結核には無効であると言われている抗結核薬イソニアジドに耐性を示すことが明らかになっている[7]．マイクロアレイによる解析では，低酸素に移行する過程で劇的な転写のリプログラミングが観察されることから[8]，Wayne モデルは休眠菌の代謝や遺伝子発現などを研究するうえで広く用いられる．

低酸素モデルをさらに発展させ，より宿主環境を再現したモデルの開発も行われている．弱酸性条件下において一酸化窒素処理を行うことにより活性化した免疫細胞に菌が感染した状況を再現したモデル[9]や，鉄や炭素源を制限することで肉芽腫中心の乾酪壊死部分の環境を再現したモデルを用いた研究は，複数の刺激を加えることでより宿主環境内におけるストレスを反映したモデルとして報告されている[3][10]．これらのモデルを活用することにより，休眠菌にも有効な抗結核薬の開発が期待される．

休眠を制御する分子

休眠を行う際，結核菌は表層抗原や代謝を変化させることで宿主免疫系に適応していると考えられており，これまでに幾つかの分子が休眠

図1　結核菌の生活環と病態の関係およびそれぞれのステージに移行する際に発現する分子を模式図にしたもの

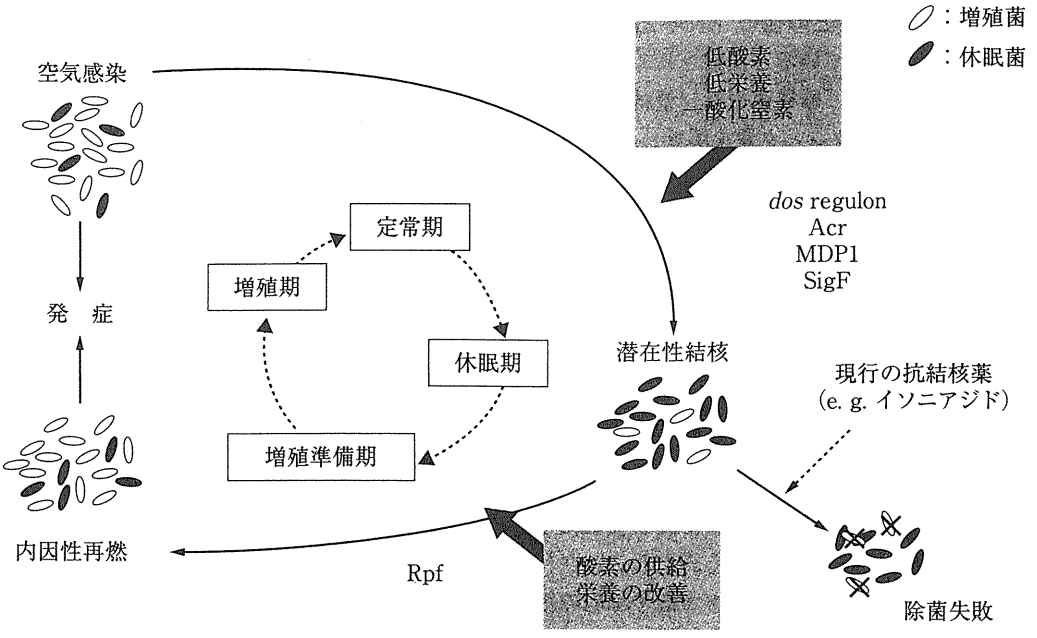

結核発症時には増殖菌が，潜在性結核の際は休眠菌が優位を占める．両方を殺傷する結核治療法がない限り，完全な除菌が不可能である．
略語：巻末の「今月の略語」参照

を制御すると報告されている（図1）．低酸素により発現が誘導される転写因子によって誘導される50程度の遺伝子群である *dos*（dormancy survival）regulon[11]には，脂肪酸合成や硝酸還元酵素をコードする遺伝子が含まれており[12]，休眠の維持に関与していると考えられている．この遺伝子群の発現上昇が起こらない変異株を用いた研究では，低酸素環境下で細胞内のATPおよびNADHレベルを維持することができず，低酸素を解除した後での休眠からの回復が遅延すると報告されている[13]．

ストレスタンパク質である16kD α–crystallin（Acr）も，定常期以降の菌体[14]や低酸素条件下[15]，マクロファージのファゴソーム内[16]などさまざまなストレス環境下で発現が誘導される分子である．Acrは低酸素環境で細胞の安定化に関与する分子であると考えられることから，低酸素による休眠導入のマーカーとして利用されている．

Mycobacterium smegmatis のヒストン様タンパク質の1つであるHlpは，好気条件下の増殖菌体内では低濃度で存在するにもかかわらず，コールドショックおよび低酸素により発現が誘導されることが明らかになっている[17]．興味深いことに，*Streptomyces coelicolor* のHlpホモログであるHupSは，芽胞形成時に発現が上昇する分子として報告されている[18]．HupSは核様体タンパク質であり，芽胞内の染色体の安定化とストレス防御に関与していると考えられている．抗酸菌のHlpも核様体タンパク質であり，試験管内でもDNAと強固に結合することが知られているが，Hlp欠失株は野生株同様に増殖することが可能であり，コールドショック[19]や低酸素[17]の影響も受けないこと

が報告されていることから，ストレス環境下における抗酸菌のクロマチン構造の安定化にはLsr2[20]やDps[21]などの他のDNA結合タンパク質なども関与していると推察される．

一方，松本らは，結核菌やウシ型結核菌弱毒株の静止期の主要タンパク質を解析したところ，GC豊富領域核酸（DNAとRNA）に結合するDNA結合性タンパク質であることを見いだし，mycobacterial DNA-binding protein 1（MDP1）と名づけた[22]．MDP1はHlpのホモログであったが，転写や翻訳を抑制して菌の増殖停止を促す活性があることを明らかにした[23]．MDP1は結核菌の増殖制御や休眠現象に深くかかわる分子と考えられ[24]，この仮説はドイツのグループからも実験的に支持されている[25]．

さまざまな環境の変化によって発現する転写制御因子の中にも，休眠と深くかかわるとされるものが報告されている．シグマ因子は他の細菌において芽胞形成を制御する分子として研究されており，抗酸菌においても休眠時に発現が上昇することが報告されている．例えばSigFは高病原性の遅育抗酸菌にのみ観察される分子であるが[26]，マクロファージへの感染時[27]や長期培養時[28]などのストレス環境下において，この分子をコードする遺伝子の転写が増強することが報告されている．その一方で，SigF欠失株は微好気環境や長期培養時でも野生株と生存率に差がないことが明らかになっている[29]．また，SigF欠失株はマクロファージ内での生存に関与するとされるAcrの発現が抑制されているにもかかわらず，細胞内での生存率に野生株との差が認められないことも明らかにされている[30]．

休眠の解除を制御する分子

休眠からの再燃（resuscitation）は，増殖を停止し代謝を抑制した状態である休眠菌が，環境の変化に伴って活発な代謝活動および増殖を再開する現象である．抗酸菌において，再燃は細胞外に分泌された分子がシグナルとして働いた結果誘導されると言われている．*Micrococcus luteus*の分泌タンパク質であるresuscitation promoting factor（Rpf）には，実験モデルで作製した休眠抗酸菌の再増殖を促す能力が報告されており，抗酸菌のRpfホモログにも同様の作用があることが明らかになっている[31]．また，抗酸菌Rpfの組み換えタンパク質は凍結乾燥したBCG菌体の再増殖を促進し[32]，結核患者の喀痰からの分離生菌数を増加させる[33]．抗酸菌には5つのRpfパラログが存在しており，結晶構造解析から，5つの分子に共通な領域がc型リソザイム様の構造を有し，細胞壁ペプチドグリカンの成分であるN-アセチルグルコサミンとN-アセチルムラミン酸間のグリコシド結合を切断する酵素として機能することが推定された[34]．細胞壁成分であるペプチドグリカンの破壊は菌の薬剤感受性の増強を引き起こすとされており，実際にRpfパラログの幾つかを欠失した株ではドデシル硫酸ナトリウム（SDS）に対する感受性の増強が認められる[35]．

一方，芽胞から発芽して栄養型になる際，ペプチドグリカンの加水分解による細胞壁の破壊は必須であり，*Bacillus anthracis*の有する幾つかの加水分解酵素の欠失株では，芽胞形成は正常であるにもかかわらず出芽の異常が認められる[36]．ペプチドグリカンの分解によって生じるムロペプチドには，シグナル伝達分子として働く機能も報告されており，ムロペプチドの添加により*Bacillus*属の発芽が促進されたという研究報告もなされている[37]．結核菌においては，5つのRpf分子のうち再燃に必須な分子はどれかという議論についてはさまざまな相反するデータが報告されているが[35][38]，いまだ全体で一致した結論には至っておらず，結核菌における再燃の誘導には複数の異なる経路が存在するのではないかと推察されている．

ま と め

結核菌は，宿主内で増殖/休眠/再燃という不均一な状態で感染している．増殖/休眠/再燃菌

の存在比率は，感染した宿主の免疫能および薬剤治療の前後によって大きく異なると推察されるため，それぞれの条件を適切に再現する複数の実験モデルの構築は，各ステージにおいて最も優勢にあるポピュレーションを効果的に殺菌する抗結核薬の開発において必要であると考えられる．また，それぞれのステージにおいて特異的に発現される分子の特定は，結核に罹患した患者が現在どのステージに置かれているかを診断するうえで有効なプローブになると期待される．

最初に述べたように，結核菌の住み処はヒトに限定されているため，ヒトに寄生する結核菌，すなわち活動性結核に加え潜在性結核に対処することが結核の制圧に繋がる．また，休眠という長期間の生命維持機構の解明が，ヒトの長寿にも応用できる成果となれば幸いに思う．

謝 辞

紹介した我々の研究は，文部科学省科学研究費，厚生労働省科学研究費，ヒューマンサイエンス振興財団により支援された．

文　　献

1) Loebel R O, et al: The Influence of Adverse Conditions upon the Respiratory Metabolism and Growth of Human Tubercle Bacilli. J Bacteriol 26 (2): 167–200, 1933.
2) Smeulders M J, et al: Adaptation of *Mycobacterium smegmatis* to stationary phase. J Bacteriol 181 (1): 270–283, 1999.
3) Betts J C, et al: Evaluation of a nutrient starvation model of *Mycobacterium tuberculosis* persistence by gene and protein expression profiling. Mol Microbiol 43 (3): 717–731, 2002.
4) Via L E, et al: Tuberculous granulomas are hypoxic in guinea pigs, rabbits, and nonhuman primates. Infect Immun 76 (6): 2333–2340, 2008.
5) Wayne L G: Dynamics of submerged growth of *Mycobacterium tuberculosis* under aerobic and microaerophilic conditions. Am Rev Respir Dis 114 (4): 807–811, 1976.
6) Wayne L G, et al: An *in vitro* model for sequential study of shiftdown of *Mycobacterium tuberculosis* through two stages of nonreplicating persistence. Infect Immun 64 (6): 2062–2069, 1996.
7) Wayne L G, et al: Metronidazole is bactericidal to dormant cells of *Mycobacterium tuberculosis*. Antimicrob Agents Chemother 38 (9): 2054–2058, 1994.
8) Muttucumaru D G, et al: Gene expression profile of *Mycobacterium tuberculosis* in a non-replicating state. Tuberculosis (Edinb) 84 (3–4): 239–246, 2004.
9) Bryk R, et al: Selective killing of nonreplicating mycobacteria. Cell Host Microbe 3 (3): 137–145, 2008.
10) Rifat D, et al: Phosphate depletion: a novel trigger for *Mycobacterium tuberculosis* persistence. J Infect Dis 200 (7): 1126–1135, 2009.
11) Voskuil M I, et al: *Mycobacterium tuberculosis* gene expression during adaptation to stationary phase and low-oxygen dormancy. Tuberculosis (Edinb) 84 (3–4): 218–227, 2004.
12) Voskuil M I, et al: Inhibition of respiration by nitric oxide induces a *Mycobacterium tuberculosis* dormancy program. J Exp Med 198 (5): 705–713, 2003.
13) Leistikow R L, et al: The *Mycobacterium tuberculosis* DosR regulon assists in metabolic homeostasis and enables rapid recovery from nonrespiring dormancy. J Bacteriol 192 (6): 1662–1670, 2010.
14) Yuan Y, et al: Stationary phase-associated protein expression in *Mycobacterium tuberculosis*: function of the mycobacterial alpha-crystallin homolog. J Bacteriol 178 (15): 4484–4492, 1996.
15) Cunningham A F, et al: Mycobacterial stationary phase induced by low oxygen tension: cell wall thickening and localization of the 16-kilodalton alpha-crystallin homolog. J Bacteriol 180 (4): 801–808, 1998.
16) Monahan I M, et al: Differential expression of mycobacterial proteins following phagocytosis by macrophages. Microbiology 147 (Pt 2): 459–

471, 2001.
17) Lee B H, et al: Upregulation of a histone-like protein in dormant *Mycobacterium smegmatis*. Mol Gen Genet 260 (5): 475-479, 1998.
18) Salerno P, et al: One of the two genes encoding nucleoid-associated HU proteins in *Streptomyces coelicolor* is developmentally regulated and specifically involved in spore maturation. J Bacteriol 191 (21): 6489-6500, 2009.
19) Shires K, et al: The cold-shock stress response in *Mycobacterium smegmatis* induces the expression of a histone-like protein. Mol Microbiol 39 (4): 994-1009, 2001.
20) Colangeli R, et al: The multifunctional histone-like protein Lsr2 protects mycobacteria against reactive oxygen intermediates. Proc Natl Acad Sci USA 106 (11): 4414-4418, 2009.
21) Gupta S, et al: Proteomics analysis of carbon-starved *Mycobacterium smegmatis*: induction of Dps-like protein. Protein Eng 15 (6): 503-512, 2002.
22) Matsumoto S, et al: Identification of a novel DNA-binding protein from *Mycobacterium bovis* bacillus Calmette-Guérin. Microbiol Immunol 43 (11): 1027-1036, 1999.
23) Matsumoto S, et al: The gene encoding mycobacterial DNA-binding protein I (MDPI) transformed rapidly growing bacteria to slowly growing bacteria. FEMS Microbiol Lett 182 (2): 297-301, 2000.
24) Katsube T, et al: Control of cell wall assembly by a histone-like protein in mycobacteria. J Bacteriol 189 (22): 8241-8249, 2007.
25) Lewin A, et al: The mycobacterial DNA-binding protein 1 (MDP1) from *Mycobacterium bovis* BCG influences various growth characteristics. BMC Microbiol 8: 91, 2008.
26) DeMaio J, et al: A stationary-phase stress-response sigma factor from *Mycobacterium tuberculosis*. Proc Natl Acad Sci USA 93 (7): 2790-2794, 1996.
27) Graham J E, et al: Identification of *Mycobacterium tuberculosis* RNAs synthesized in response to phagocytosis by human macrophages by selective capture of transcribed sequences (SCOTS). Proc Natl Acad Sci USA 96 (20): 11554-11559, 1999.
28) Manganelli R, et al: Differential expression of 10 sigma factor genes in *Mycobacterium tuberculosis*. Mol Microbiol 31 (2): 715-724, 1999.
29) Chen P, et al: Construction and characterization of a *Mycobacterium tuberculosis* mutant lacking the alternate sigma factor gene, sigF. Infect Immun 68 (10): 5575-5580, 2000.
30) Yuan Y, et al: The 16-kDa alpha-crystallin (Acr) protein of *Mycobacterium tuberculosis* is required for growth in macrophages. Proc Natl Acad Sci USA 95 (16): 9578-9583, 1998.
31) Mukamolova G V, et al: A family of autocrine growth factors in *Mycobacterium tuberculosis*. Mol Microbiol 46 (3): 623-635, 2002.
32) Wu X, et al: Effect of recombinant Rv1009 protein on promoting the growth of *Mycobacterium tuberculosis*. J Appl Microbiol 105 (4): 1121-1127, 2008.
33) Mukamolova G V, et al: Resuscitation-promoting factors reveal an occult population of tubercle Bacilli in Sputum. Am J Respir Crit Care Med 181 (2): 174-180, 2010.
34) Cohen-Gonsaud M, et al: The structure of a resuscitation-promoting factor domain from *Mycobacterium tuberculosis* shows homology to lysozymes. Nat Struct Mol Biol 12 (3): 270-273, 2005.
35) Kana B D, et al: The resuscitation-promoting factors of *Mycobacterium tuberculosis* are required for virulence and resuscitation from dormancy but are collectively dispensable for growth *in vitro*. Mol Microbiol 67 (3): 672-684, 2008.
36) Giebel J D, et al: The germination-specific lytic enzymes SleB, CwlJ1, and CwlJ2 each contribute to *Bacillus anthracis* spore germination and virulence. J Bacteriol 191 (18): 5569-5576, 2009.
37) Shah I M, et al: A eukaryotic-like Ser/Thr kinase signals bacteria to exit dormancy in response to peptidoglycan fragments. Cell 135

(3): 486–496, 2008.
38) Russell–Goldman E, et al: A *Mycobacterium tuberculosis* Rpf double–knockout strain exhibits profound defects in reactivation from chronic tuberculosis and innate immunity phenotypes. Infect Immun 76 (9): 4269–4281, 2008.

Current Research on Tuberculosis
–Latent *Mycobacterium tuberculosis* Infection (LTBI) and *M. tuberculosis*: Molecular Mechanism of Dormancy–

Mamiko Niki[1], Makoto Niki[1], Yuriko Ozeki[1,2],
Mayuko Osada–Oka[1], Sohkichi Matsumoto[1]
[1] Department of Bacteriology, Osaka City University Graduate School of Medicine
[2] Department of Food and Nutrition, Faculty of Human Health,
Sonoda Women's University

Biochemical and Biophysical Research Communications 409 (2011) 304–307

Contents lists available at ScienceDirect

Biochemical and Biophysical Research Communications

journal homepage: www.elsevier.com/locate/ybbrc

Glycerol monomycolate, a latent tuberculosis-associated mycobacterial lipid, induces eosinophilic hypersensitivity responses in guinea pigs

Yuki Hattori [a,b], Isamu Matsunaga [a,b], Takaya Komori [a,b], Tetsuo Urakawa [a,b], Takashi Nakamura [c], Nagatoshi Fujiwara [d], Kenji Hiromatsu [e], Hideyoshi Harashima [c], Masahiko Sugita [a,b,*]

[a] Laboratory of Cell Regulation, Institute for Virus Research, Kyoto University, Kyoto 606-8507, Japan
[b] Laboratory of Cell Regulation and Molecular Network, Graduate School of Biostudies, Kyoto University, Kyoto 606-8501, Japan
[c] Faculty of Pharmaceutical Sciences, Hokkaido University, Sapporo 060-0812, Japan
[d] Department of Bacteriology, Osaka City University Graduate School of Medicine, Osaka 545-8585, Japan
[e] Department of Microbiology and Immunology, Faculty of Medicine, Fukuoka University, Fukuoka 814-0180, Japan

ARTICLE INFO

Article history:
Received 18 April 2011
Available online 7 May 2011

Keywords:
Glycerol monomycolate
Latent infection
BCG

ABSTRACT

Dynamic changes in the lipid composition of the cell wall occur in pathogenic mycobacteria that are often intended for adaptation to the host environment. Dormant mycobacteria should have evolved efficient maneuvers for cohabitation, allowing the microbes to persist for years within the host. Glycerol monomycolate (GroMM) has been implicated as a specific immune target in human individuals with latent, but not active, tuberculosis, but the *in vivo* response to GroMM and the relevance of it to latent infection remain poorly understood. Here, we immunized guinea pigs with bacillus Calmette–Guerin (BCG) expressing high levels of GroMM and then, monitored skin reactions at the site of challenge with GroMM-containing liposome. We found that BCG-immunized guinea pigs mounted enhanced skin reactions to GroMM with prominent local infiltration by eosinophils. Consistent with this, GroMM-stimulated lymph node cells upregulated the expression of T helper (Th)2-type cytokines, such as interleukin (IL)-5 and IL-10, that could potentially counteract the microbe-eliminating Th1-type cytokine response. On the basis of these observations, we predict that the host response to GroMM produced by dormant mycobacteria would contribute to their long-term survival in the host.

1. Introduction

Mycobacterium tuberculosis, a causative microorganism of human tuberculosis, and other mycobacteria species possess highly lipid-rich cell walls that are critical not simply for their acid-fast properties but also for their survival and virulence. The cell wall contains mycolic acids (MA), a family of α-alkyl-β-hydroxy fatty acids with extremely long carbon-chains, that are densely aligned in association with surface-exposed glycolipids, thereby forming the hydrophobic cell wall architecture. Among the surface-exposed glycolipids, trehalose dimycolate (TDM) has long been thought to be a major glycosylmycolate, but our recent studies have indicated that the efficiency of TDM biosynthesis varies significantly among mycobacteria species [1]. More strikingly, the lipid composition of the cell wall of mycobacteria can be altered dynamically in response to external factors present either in culture media or in host cells [2]. The identification of specific lipid species produced by mycobacteria in infected hosts as well as the analysis of the host response directed toward them will provide important new insights into host-microbe interactions in human tuberculosis, a major global health issue that requires further efforts for prevention and treatment.

It is estimated that about one third of the world population is infected with *M. tuberculosis*, but most infected individuals remain free of apparent disease manifestations. This persistent subclinical infection is referred to as latent infection, in which the microbes survive silently in host cells without replication. Because of the suppressed overall metabolism, these dormant mycobacteria are unlikely to produce cell wall lipids at a level comparable with that for actively replicating microbes, but a recent study has identified GroMM as a mycobacterial lipid species potentially associated with latent infection [3]. Unlike TDM [4] and other MA-containing glycolipids [5–7], GroMM has not been a common target of research, and the host-response to GroMM as well as its relevance to latent infection remains to be addressed.

Abbreviations: BCG, *M. bovis* bacillus Calmette–Guerin; GAPDH, glyceraldehyde-3-phosphate dehydrogenase; GroMM, glycerol monomycolate; IFN, interferon; IL, interleukin; MA, mycolic acid; MN, mononuclear; PMN, polymorphonuclear; TDM, trehalose dimycolate; Th, T helper; TLC, thin layer chromatography.

* Corresponding author at: Laboratory of Cell Regulation, Institute for Virus Research, Kyoto University, Kyoto 606-8507, Japan. Fax: +81 75 752 3232.
E-mail address: msugita@virus.kyoto-u.ac.jp (M. Sugita).

0006-291X/$ - see front matter © 2011 Elsevier Inc. All rights reserved.
doi:10.1016/j.bbrc.2011.04.146

Here, we first established a method for obtaining BCG expressing high levels of GroMM, and then assessed cutaneous responses in the GroMM-challenged skin of GroMM^{high} BCG-immunized guinea pigs. We found that, whereas GroMM was capable of inducing local infiltration by eosinophils in unsensitized guinea pigs, the eosinophilic response was even more enhanced in sensitized animals, which were associated with upregulated expression of IL-5 and IL-10 in draining lymph nodes. As these cytokines counteract the Th1-type response that is critical for clearing infection with *M. tuberculosis*, the GroMM-elicited response may favor the microbe's persistence in the host.

2. Materials and methods

2.1. Chemical reagents, bacteria culture, and lipid analysis

Chemical reagents were purchased from Nacalai Tesque (Kyoto, Japan) unless otherwise indicated. The BCG Tokyo 172 strain was kindly provided by Dr. Ikuya Yano (Japan BCG Laboratory, Tokyo, Japan) and grown in the Middlebrook 7H9 medium supplemented with the ADC enrichment (BD Biosciences, Franklin Lakes, NJ) and indicated concentrations of glycerol. The bacteria were harvested when the optical density at 600 nm reached 1–1.5, and lipids were extracted with chloroform/methanol as described previously [8,9]. The lipid samples were then fractionated by two cycles of thin layer chromatography (TLC) using an Analtech TLC plate (Newark, DE) with a solvent system of chloroform/ethyl acetate (5:1). In some experiments, the spot comigrating with the GroMM reference was extracted and purified, followed by mass spectrometric analysis according to the method described previously [10].

2.2. Liposome preparation

The stearylated octaarginine-containing liposome was generated as described previously [6,11,12] with slight modifications adapted for the integration of GroMM. Briefly, purified GroMM in chloroform was mixed with egg phosphatidylcholine (NOF Corp., Tokyo Japan), cholesterol (Avanti Polar Lipids, Alabaster, AL), and stearylated octaarginine (KURABO, Osaka, Japan) at a molar ratio of 7:3:0.5 in a test tube, and a lipid film was prepared by evaporating the solvent. The lipid film was then hydrated by adding distilled water, and the mixture was sonicated gently for liposome formation. The efficiency of GroMM integration into the liposome was 65%, as determined by TLC-based resolution of the liposome components. The diameter and ζ-potential of the liposome were 148 nm and 49 mV, respectively.

2.3. Animals and skin tests

Three-week-old female Hartley guinea pigs were purchased from Japan SLC, Inc. (Shizuoka, Japan), and housed under specific pathogen-free conditions. BCG was grown in 5% glycerol-containing 7H9 medium and harvested at its mid-log phase growth. Immunization of guinea pigs with BCG and skin tests were performed as established in our previous studies using other mycolylglycolipid antigens [6,13]. Briefly, the BCG bacteria (1×10^8 colony-forming units) were injected intradermally, and after 8 weeks, liposome containing 5 μg of GroMM as well as an equivalent amount of empty liposome was dissolved in 100 μl of phosphate-buffered saline and injected subcutaneously. After the injection, the skin response was monitored at the indicated time points by measuring the distance across the skin induration. All animal experiments were performed according to the institutional guidelines on animal welfare and humane treatment of laboratory animals.

2.4. Histochemistry

The excised skin samples were fixed for 1 day with 4% paraformaldehyde, dehydrated, and embedded in paraffin. The tissue sections were stained with Giemsa's stain solution, and observed under a microscope. The numbers of mononuclear (MN) cells, polymorphonuclear (PMN) cells as well as eosinophils were determined in ten randomly selected high power fields, and statistical analysis was performed.

2.5. RT-PCR

Inguinal lymph node cells were isolated from BCG-immunized guinea pigs. The cells (2×10^6/well) were placed in wells of 96-well tissue culture plates and stimulated with either GroMM in liposome (1 μg/ml) or empty liposome in RPMI1640 medium (Invitrogen, Carlsbad, CA) supplemented with 10% heat-inactivated fetal calf serum (Hyclone, Logan, UT). After 18 h at 37 °C, the cells were harvested, and total RNA was extracted using the RNeasy mini kit (Qiagen, Hilden Germany). The first-strand cDNA was synthesized from approximately 0.1 μg of total RNA using oligo(dT) and the PrimeScript reverse transcriptase (Takara Bio, Inc., Otsu, Japan). To amplify specific transcripts, the samples were subjected to PCR for 35 cycles of 1 min at 94 °C, 1 min at 60 °C, and 1 min at 72 °C followed by a 10-min incubation at 72 °C. The primers used were: 5′-CTA GCT ACT ACT GCC AGT CAA GAT-3′ (sense) and 5′-GCT CTG AAA CAG CAT CTG AGT CCT-3′ (antisense) for interferon (IFN)-γ; 5′-CCA TGA GGG TGC TTC TGC AGT TGG G-3′ (sense) and 5′-CTC AGC CTT CAA TTG TCC ATT CCG T-3′ (antisense) for IL-5; 5′-GGC ACG AAC ACC CAG TCT GA-3′ (sense) and 5′-TCA CCT GCT CCA CTG CCT TG-3′ (antisense) for IL-10; 5′-GAT ATT GTA GCC ATC AAT GAT CCC T-3′ (sense) and 5′-CAT CGT ATT TGG CCG GTT TCT AG-3′ (antisense) for glyceraldehyde-3-phosphate dehydrogenase (GAPDH). The PCR products were resolved on 1.2% agarose gels and visualized by staining with ethidium bromide and UV transillumination.

2.6. Statistical analysis

The statistical analysis was performed using Student's *t* test.

3. Results and discussion

3.1. Induction of GroMM biosynthesis in cultured mycobacteria

BCG grown in standard 7H9 media does not produce readily detectable levels of GroMM. The metabolic pathway for the biosynthesis of GroMM is poorly understood, but we predicted that supplementation of excess glycerol might promote its production. We therefore cultured BCG in the 7H9 medium containing increasing concentrations of glycerol, and lipids extracted from the bacteria were fractionated by TLC. As expected, GroMM was undetectable in BCG cultured without glycerol, but the amount of a lipid species comigrating with the GroMM reference increased in a glycerol concentration-dependent manner (Fig. 1A, indicated with an arrow). Matrix-assisted laser desorption/ionization time-of-flight mass spectrometric analysis of the purified lipid species revealed that the mass numbers of given ions were matched with those of sodium adducts of GroMM containing either C78:2 α-MA (*m/z*, 1234), C80:2 α-MA (*m/z*, 1262), C82:1 keto-MA (*m/z*, 1306), C82:1 methoxy-MA (*m/z*, 1322), C84:1 keto-MA (*m/z*, 1334), C84:1 methoxy-MA (*m/z*, 1350), C86:1 keto-MA (*m/z*, 1362), C87:1 keto-MA (*m/z*, 1376) or C88:1 keto-MA (*m/z*, 1390) (Fig. 1B). On the basis of these observations, we concluded that BCG expressing high levels of GroMM

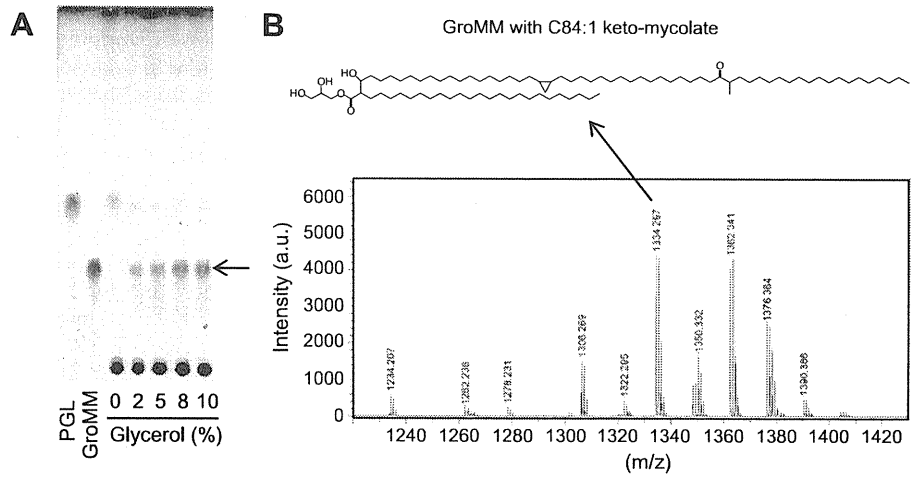

Fig. 1. GroMM expression in cultured BCG. (A) BCG was cultured in the 7H9 medium containing indicated concentrations of glycerol, and the extracted lipids were analyzed by TLC. The position of GroMM is indicated with an arrow. PGL, phenolic glycolipid. (B) Matrix-assisted laser desorption/ionization time-of-flight mass spectrometry profiles of the purified lipid that comigrated with the GroMM reference and the structure of GroMM with C84:1 keto-mycolate (*m/z*, 1334) are shown.

was readily available by culturing the microbes in glycerol-rich medium.

3.2. GroMM-elicited eosinophilic skin reactions

Our initial studies using BCG cultured in the standard 7H9 medium failed to induce high levels of GroMM-specific immune responses in immunized subjects. We reasoned that the alternative use of the GroMM^{high} BCG could potentially augment the magnitude of host responses directed against GroMM, allowing us to assess the quality of the specific response. We therefore analyzed GroMM-elicited skin responses in GroMM^{high} BCG-immunized guinea pigs. Whereas mock-treated guinea pigs elicited low levels of skin responses at the site of antigen challenge (Fig. 2, upper panel), those immunized with GroMM^{high} BCG began to develop detectable induration as early as 12 h after challenge, and the response was much more pronounced in magnitude compared with that observed in mock-treated animals (Fig. 2, lower panel). Histochemical analysis of the skin challenged with GroMM liposome in GroMM^{high} BCG-immunized guinea pigs revealed significant infiltration by PMN cells (Fig. 3 D and E), most of which were eosinophils (Fig. 3D, inset, and 3E). A similar pattern of response was observed for the GroMM liposome-challenged skin of mock-treated animals, but the response was significantly milder compared with that in GroMM^{high} BCG-immunized subjects (Fig. 3 B and E). The number of MN cells infiltrating into the GroMM liposome-

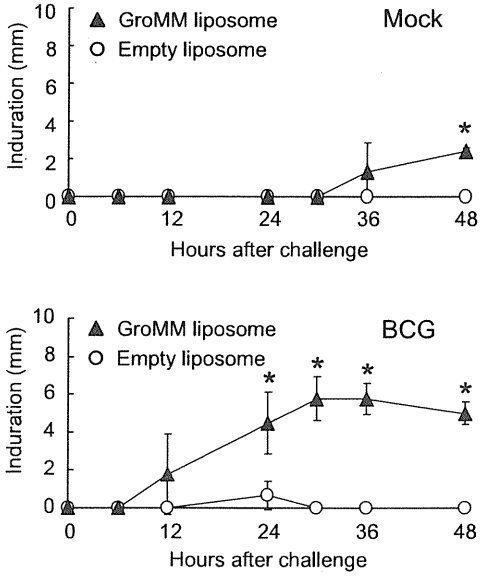

Fig. 2. GroMM-elicited skin responses in BCG-immunized guinea pigs. GroMM^{high} BCG-immunized (lower panel) and mock-treated (upper panel) guinea pigs ($n = 4$ for each group) received intradermal injection of either GroMM liposome (filled triangles) or empty liposome (open circles), and the skin induration was monitored at indicated time points. *$p < 0.01$.

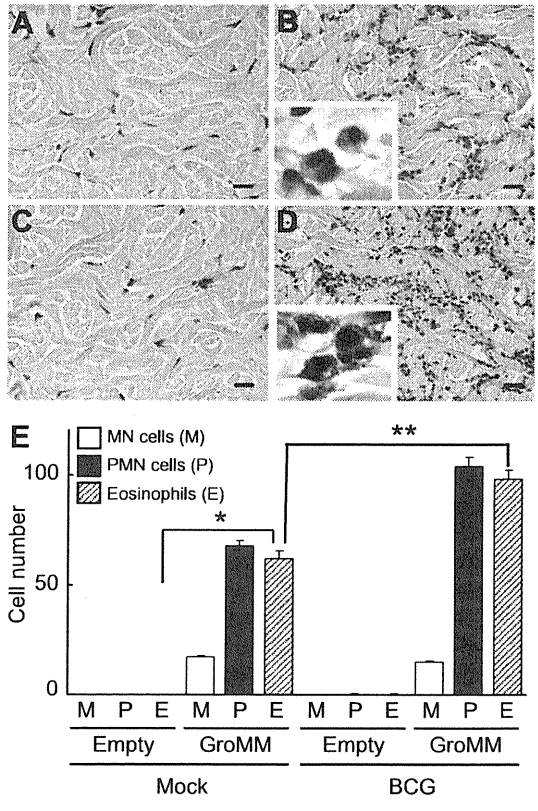

Fig. 3. Eosinophilic hypersensitivity response in GroMM-challenged skin. GroMM-^{high} BCG-immunized (C, D) and mock-treated guinea pigs (A, B) received intradermal injection of either GroMM liposome (B, D) or empty liposome (A, C), and after 2 days, the excised skin samples were subjected to Giemsa's staining. The magnified views of the infiltrating eosinophils are shown in insets (B, D). Scale bars, 50 μm. The numbers of infiltrating MN cells (M), PMN cells (P), and eosinophils (E) are shown in panel E. *$p < 0.01$, **$p < 0.01$.

challenged skin was comparable between GroMM^{high} BCG-immunized and mock-treated guinea pigs (Fig. 3E). No apparent response was observed when the skin was challenged with empty liposome (Fig. 3 A and C), indicating that the skin response elicited by GroMM liposome was not due to non-specific stimulation by liposome components, such as phosphatidylcholine and cholesterol. These results detected for the first time the eosinophilic hypersensitivity response directed against GroMM.

3.3. Upregulated IL-5 and IL-10 transcription in GroMM-stimulated lymph node cells

Eosinophilic hypersensitivity responses induced in sensitized subjects are often associated with skewed production of Th2-type cytokines [13]. Indeed, draining lymph node cells obtained from GroMM^{high} BCG-immunized guinea pigs upregulated IL-5 and IL-10 mRNA transcription upon *in vitro* stimulation with GroMM liposome (Fig. 4). The expression of IFN-γ mRNA was observed even in unstimulated lymph node cells, which was likely due to activation *in vivo* in inflamed lymph nodes, and its transcription was slightly downregulated in GroMM liposome-stimulated cells. Thus, the GroMM-elicited eosinophilic hypersensitivity response was associated with upregulated expression of IL-5 and IL-10 cytokines, capable of activating eosinophils and suppressing the Th1-type cytokine response, respectively.

The present study and a series of our previous studies [2,6,13] highlight dynamic adaptation strategies that have been evolved after a long-term interaction and cohabitation between humans and *M. tuberculosis*. Mycobacteria grown in the environment biosynthesize TDM, but TDM should be downregulated for the microbes to survive within the host because of its highly potent adjuvancy [13,14]. Upon entry into the host, pathogenic mycobacteria employ a smart strategy for TDM downregulation by using host-derived glucose as an alternative substrate for their mycolyltransferases [2]. This enzymatic reaction, however, results in unintended generation of a new T-cell antigen, glucose monomycolate (GMM), recognized by the host cytotoxic T cells [15,16]. The hypersensitivity response to GMM is highly skewed to Th1-type cytokine production that efficiently supports elimination of the microbes [6]. Therefore, it is reasonable to speculate that dormant mycobacteria capable of surviving for years in host cells may have downregulated the expression of both TDM and GMM. Indeed, artificial dormant mycobacteria obtained from the Wayne model [17] did not express these mycolylglycolipids at a level comparable with that for growing microbes (data not shown). GroMM, identified as an immune target in individuals with latent tuberculosis [3], might function to compensate for the loss of TDM and GMM and maintain the integrity of the cell wall. Our present study further underscores that the switch from GMM to GroMM could dynamically change the type of host responses from Th1 to Th2, providing the dormant mycobacteria with a valuable opportunity to persist in host cells. Thus, this study has important medical implications, including diagnosis and treatment of latent tuberculosis.

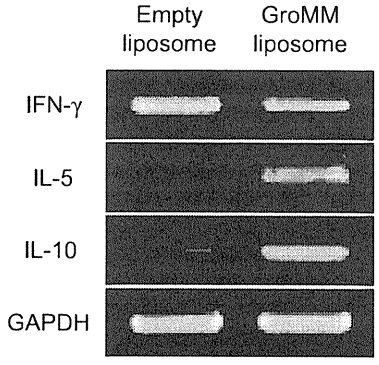

Fig. 4. IL-5 and IL-10 expression by GroMM-stimulated lymph node cells. Draining lymph node cells isolated from GroMM^{high} BCG-immunized guinea pigs were stimulated *in vitro* either with GroMM liposome or with empty liposome. After 18 h, RNA was extracted and RT-PCR was performed to detect IFN-γ, IL-5, IL-10 and GAPDH transcripts.

Acknowledgments

We thank Dr. Ikuya Yano for providing the BCG Tokyo 172 strain. This work was supported by grants from the Japan Society for the Promotion of Science (Grant-in-Aid for Scientific Research(B)) and from the Ministry of Health, Labour, and Welfare (Research on Emerging and Re-emerging infectious Diseases).

References

[1] H. Nakao, I. Matsunaga, D. Morita, T. Aboshi, T. Harada, Y. Nakagawa, N. Mori, M. Sugita, Mycolyltransferase from *Mycobacterium leprae* excludes mycolate-containing glycolipid substrates, J. Biochem. 146 (2009) 659–665.
[2] I. Matsunaga, T. Naka, R.S. Talekar, M.J. McConnell, K. Katoh, H. Nakao, A. Otsuka, S.M. Behar, I. Yano, D.B. Moody, M. Sugita, Mycolyltransferase-mediated glycolipid exchange in Mycobacteria, J. Biol. Chem. 283 (2008) 28835–28841.
[3] E. Layre, A. Collmann, M. Bastian, S. Mariotti, J. Czaplicki, J. Prandi, L. Mori, S. Stenger, G. De Libero, G. Puzo, M. Gilleron, Mycolic acids constitute a scaffold for mycobacterial lipid antigens stimulating CD1-restricted T cells, Chem. Biol. 16 (2009) 82–92.
[4] E. Ishikawa, T. Ishikawa, Y.S. Morita, K. Toyonaga, H. Yamada, O. Takeuchi, T. Kinoshita, S. Akira, Y. Yoshikai, S. Yamasaki, Direct recognition of the mycobacterial glycolipid, trehalose dimycolate, by C-type lectin Mincle, J. Exp. Med. 206 (2009) 2879–2888.
[5] T. Kawashima, Y. Norose, Y. Watanabe, Y. Enomoto, H. Narazaki, E. Watari, S. Tanaka, H. Takahashi, I. Yano, M.B. Brenner, M. Sugita, Cutting edge: major CD8 T cell response to live bacillus Calmette–Guerin is mediated by CD1 molecules, J. Immunol. 170 (2003) 5345–5348.
[6] T. Komori, T. Nakamura, I. Matsunaga, D. Morita, Y. Hattori, H. Kuwata, N. Fujiwara, K. Hiromatsu, H. Harashima, M. Sugita, A microbial glycolipid functions as a new class of target antigen for delayed-type hypersensitivity, J. Biol. Chem. 286 (2011) 16800–16806.
[7] I. Matsunaga, S. Oka, T. Inoue, I. Yano, Mycolyl glycolipids stimulate macrophages to release a chemotactic factor, FEMS Microbiol. Lett. 55 (1990) 49–53.
[8] K. Hiromatsu, C.C. Dascher, K.P. LeClair, M. Sugita, S.T. Furlong, M.B. Brenner, S.A. Porcelli, Induction of CD1-restricted immune responses in guinea pigs by immunization with mycobacterial lipid antigens, J. Immunol. 169 (2002) 330–339.
[9] I. Matsunaga, A. Bhatt, D.C. Young, T.Y. Cheng, S.J. Eyles, G.S. Besra, V. Briken, S.A. Porcelli, C.E. Costello, W.R. Jacobs Jr., D.B. Moody, *Mycobacterium tuberculosis* pks12 produces a novel polyketide presented by CD1c to T cells, J. Exp. Med. 200 (2004) 1559–1569.
[10] Y. Enomoto, M. Sugita, I. Matsunaga, T. Naka, A. Sato, T. Kawashima, K. Shimizu, H. Takahashi, Y. Norose, I. Yano, Temperature-dependent biosynthesis of glucose monomycolate and its recognition by CD1-restricted T cells, Biochem. Biophys. Res. Commun. 337 (2005) 452–456.
[11] A. Homhuan, K. Kogure, T. Nakamura, N. Shastri, H. Harashima, Enhanced antigen presentation and CTL activity by transduction of mature rather than immature dendritic cells with octaarginine-modified liposomes, J. Control. Release 136 (2009) 79–85.
[12] T. Nakamura, R. Moriguchi, K. Kogure, N. Shastri, H. Harashima, Efficient MHC class I presentation by controlled intracellular trafficking of antigens in octaarginine-modified liposomes, Mol. Ther. 16 (2008) 1507–1514.
[13] A. Otsuka, I. Matsunaga, T. Komori, K. Tomita, Y. Toda, T. Manabe, Y. Miyachi, M. Sugita, Trehalose dimycolate elicits eosinophilic skin hypersensitivity in mycobacteria-infected guinea pigs, J. Immunol. 181 (2008) 8528–8533.
[14] R. Ryll, Y. Kumazawa, I. Yano, Immunological properties of trehalose dimycolate (cord factor) and other mycolic acid-containing glycolipids – a review, Microbiol. Immunol. 45 (2001) 801–811.
[15] D.B. Moody, B.B. Reinhold, M.R. Guy, E.M. Beckman, D.E. Frederique, S.T. Furlong, S. Ye, V.N. Reinhold, P.A. Sieling, R.L. Modlin, G.S. Besra, S.A. Porcelli, Structural requirements for glycolipid antigen recognition by CD1b-restricted T cells, Science 278 (1997) 283–286.
[16] S. Stenger, R.J. Mazzaccaro, K. Uyemura, S. Cho, P.F. Barnes, J.P. Rosat, A. Sette, M.B. Brenner, S.A. Porcelli, B.R. Bloom, R.L. Modlin, Differential effects of cytolytic T cell subsets on intracellular infection, Science 276 (1997) 1684–1687.
[17] L.G. Wayne, K.Y. Lin, Glyoxylate metabolism and adaptation of *Mycobacterium tuberculosis* to survival under anaerobic conditions, Infect. Immun. 37 (1982) 1042–1049.

Cellular Microbiology (2012) doi:10.1111/j.1462-5822.2012.01754.x

Coronin-1a inhibits autophagosome formation around *Mycobacterium tuberculosis*-containing phagosomes and assists mycobacterial survival in macrophages

Shintaro Seto,[1]* Kunio Tsujimura[1] and Yukio Koide[1,2]
[1]*Department of Infectious Diseases and* [2]*Executive Director, Hamamatsu University School of Medicine, 1-20-1 Handa-yama, Higashi-ku, Hamamatsu 431-3192, Japan.*

Summary

***Mycobacterium tuberculosis* is an intracellular bacterium that can survive within macrophages. Such survival is potentially associated with Coronin-1a (Coro1a). We investigated the mechanism by which Coro1a promotes the survival of *M. tuberculosis* in macrophages and found that autophagy was involved in the inhibition of mycobacterial survival in Coro1a knock-down (KD) macrophages. Fluorescence microscopy and immunoblot analyses revealed that LC3, a representative autophagic protein, was recruited to *M. tuberculosis*-containing phagosomes in Coro1a KD macrophages. Thin-section electron microscopy demonstrated that bacilli were surrounded by the multiple membrane structures in Coro1a KD macrophages. The proportion of LC3-positive mycobacterial phagosomes colocalized with p62/SQSTM1, ubiquitin or LAMP1 increased in Coro1a KD macrophages during infection. These results demonstrate the formation of autophagosomes around *M. tuberculosis* in Coro1a KD macrophages. Phosphorylation of p38 mitogen-activated protein kinase (MAPK) was induced in response to *M. tuberculosis* infection in Coro1a KD macrophages, suggesting that Coro1a blocks the activation of the p38 MAPK pathway involved in autophagosome formation. LC3 recruitment to *M. tuberculosis*-containing phagosomes was also observed in Coro1a KD alveolar or bone marrow-derived macrophages. These results suggest that Coro1a inhibits autophagosome formation in alveolar macrophages, thereby facilitating *M. tuberculosis* survival within the lung.**

Received 13 September, 2011; revised 5 January, 2012; accepted 5 January, 2012. *For correspondence. E-mail: s-seto@hama-med.ac.jp; Tel. (+81) 53 435 2335; Fax (+81) 53 435 2335.

Introduction

Mycobacterium tuberculosis, a causative bacterium of tuberculosis, infects one-third of the world population and causes approximately 1.7 million deaths per year (World Health Organization, 2010). The ability to survive and persist in host macrophages is a major determinant of *M. tuberculosis* pathogenicity (Hingley-Wilson *et al.*, 2003). Studies suggest that this bacterium gains the ability to proliferate within infected macrophages by blocking phagolysosome biogenesis, because mycobacterial phagosomes do not fuse with lysosomal vesicles (Armstrong and Hart, 1971; Clemens and Horwitz, 1995). *M. tuberculosis* can interfere with intracellular membrane trafficking and subsequently cause phagosome maturation arrest in infected macrophages (Vergne *et al.*, 2003; 2004; Deretic *et al.*, 2004; 2006). We recently demonstrated that *M. tuberculosis* modulated the trafficking of Rab GTPases regulating phagosome maturation and that this modulation is relevant to the maturation arrest of mycobacterial phagosomes in macrophages (Seto *et al.*, 2009; 2010; 2011; Sugaya *et al.*, 2011). However, there is currently a lack of direct evidence that phagosome maturation arrest facilitates *M. tuberculosis* survival in macrophages. For example, some mutants generated by transposon mutagenesis survived and persisted within infected macrophages despite the progression of their phagosome maturation (Pethe *et al.*, 2004).

Autophagy is a unique lysosomal degradation pathway for cytoplasmic materials. This process is involved in the innate and adaptive immune systems (Deretic and Levine, 2009). The same process is also involved in the selection and exclusion of intracellular parasites especially in innate immunity and is termed xenophagy (Levine, 2005). *M. tuberculosis* is eliminated from infected macrophages by the induction of autophagy as a consequence of nutrient starvation, drug inducer or interferon-γ (Gutierrez *et al.*, 2004; Singh *et al.*, 2006). Autophagy also potentially controls the intracellular burdens of *M. tuberculosis* in macrophages (Kumar *et al.*, 2010).

These studies suggest that new therapeutic or vaccine regimens against tuberculosis might be successfully developed by targeting strategies that induce autophagy (Jagannath *et al.*, 2009; Yuk *et al.*, 2009; Jo, 2010).

Coronin-1a (Coro1a) is a member of the coronin family associated with F-actin (de Hostos, 1999) and localizes to mycobacterial phagosomes (Ferrari *et al.*, 1999). Gene silencing of Coro1a was found to prevent *M. tuberculosis* survival in macrophages (Jayachandran *et al.*, 2007; 2008; Kumar *et al.*, 2010). These results suggest that *M. tuberculosis* perverts Coro1a function to allow the survival of this bacterium in macrophages (Pieters, 2008). Currently, the survival mechanisms involved in this process are not fully understood. In this study, we found that the depletion of Coro1a promoted autophagosome formation around *M. tuberculosis*-containing phagosomes in macrophages. The molecular mechanisms of Coro1a-mediated *M. tuberculosis* survival are also discussed.

Results

Depletion of Coro1a in macrophages by siRNA prevents M. tuberculosis *survival*

To deplete Coro1a expression in Raw264.7 macrophages, we employed Coro1a-specific small interfering ribonucleic acids (siRNA) and verified the knock-down (KD) efficiency of Coro1a by immunoblot analysis. We designed two sets of the Coro1a-specific siRNA sequences, one of which is based on the report by Jayachandran *et al.* (2007). More than 90% KD efficiency for the Coro1a protein was obtained by transfection with siRNA duplexes (Fig. 1A). We then examined the survival of *M. tuberculosis* in Raw264.7 macrophages transfected with Coro1a-specific siRNA and confirmed the inhibition of *M. tuberculosis* survival in Coro1a KD macrophages (Fig. 1B) (Jayachandran *et al.*, 2007; 2008; Kumar *et al.*, 2010).

Previous studies demonstrated that lysosomes fused with mycobacterial phagosomes in Coro1a-depleted macrophages (Jayachandran *et al.*, 2007; 2008), suggesting that the inhibition of phagolysosomal biogenesis is associated with the Coro1a-dependent survival of *M. tuberculosis*.

In this study, we examined the acidification of mycobacterial phagosomes and their fusion with lysosomes in Coro1a KD macrophages (Fig. 2). Coro1a KD macrophages were infected with DsRed-expressing *M. tuberculosis* for 24 h and examined the acidification of mycobacterial phagosomes and their fusion with lysosomes by staining with LysoTracker and anti-LAMP1 antibody respectively. The proportion of LysoTracker-positive (Fig. 2A and B) and LAMP1-positive (Fig. 2C and D) mycobacterial phagosomes increased in Coro1a KD

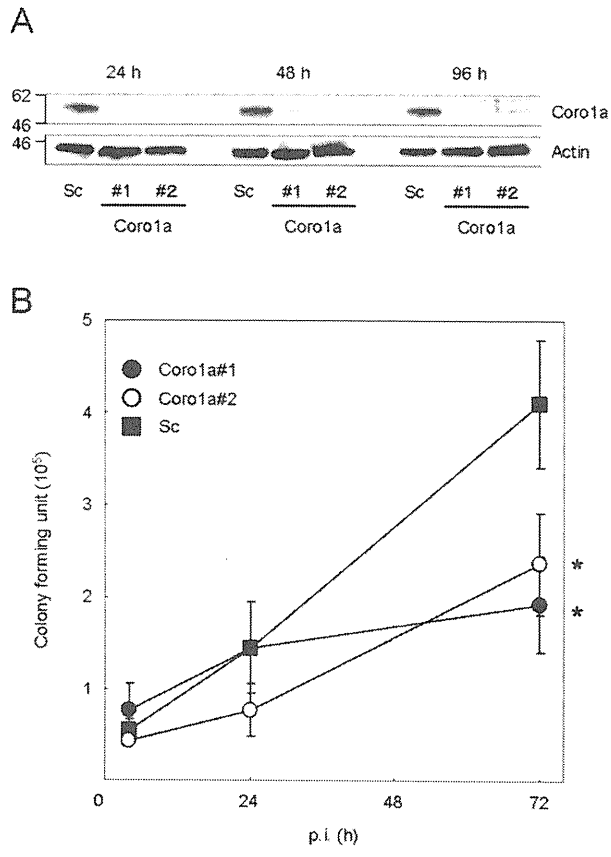

Fig. 1. Survival of *M. tuberculosis* in Coro1a KD macrophages.
A. Immunoblot analysis of Coro1a KD macrophages. Raw264.7 macrophages were transfected with Coro1a-specific or scrambled (Sc) siRNA for 24, 48 and 96 h. Whole-cell lysates from transfected macrophages were subjected to SDS-PAGE, followed by immunoblot analysis using the indicated antibodies.
B. Proliferation of *M. tuberculosis* in Coro1a KD macrophages. Macrophages were transfected with Coro1a or scrambled siRNA for 24 h and then infected with *M. tuberculosis*. The number of viable mycobacteria was determined using a colony-forming unit (cfu) assay at 4, 24 and 72 h post infection (p.i.). The data represent the means and the standard error of the means (SEM) of three independent experiments. The numbers of cfu at 72 h p.i. in macrophages transfected with Coro1a and scrambled siRNA were compared. $^*P < 0.05$ (unpaired Student's *t*-test).

macrophages. These results suggest that the maturation of mycobacterial phagosomes is promoted in Coro1a KD macrophages.

Autophagy is involved in the inhibition of M. tuberculosis *survival in Coro1a KD macrophages*

We next focused on the effect that Coro1a depletion had on the induction of autophagy in macrophages infected with *M. tuberculosis*, because autophagy is known to be associated with *M. tuberculosis* eradication (Deretic *et al.*, 2006; 2009; Jo, 2010; Lerena *et al.*, 2010). To investigate the involvement of autophagy, Coro1a KD macrophages were treated with 3-methyladenine (3-MA), an autophagy

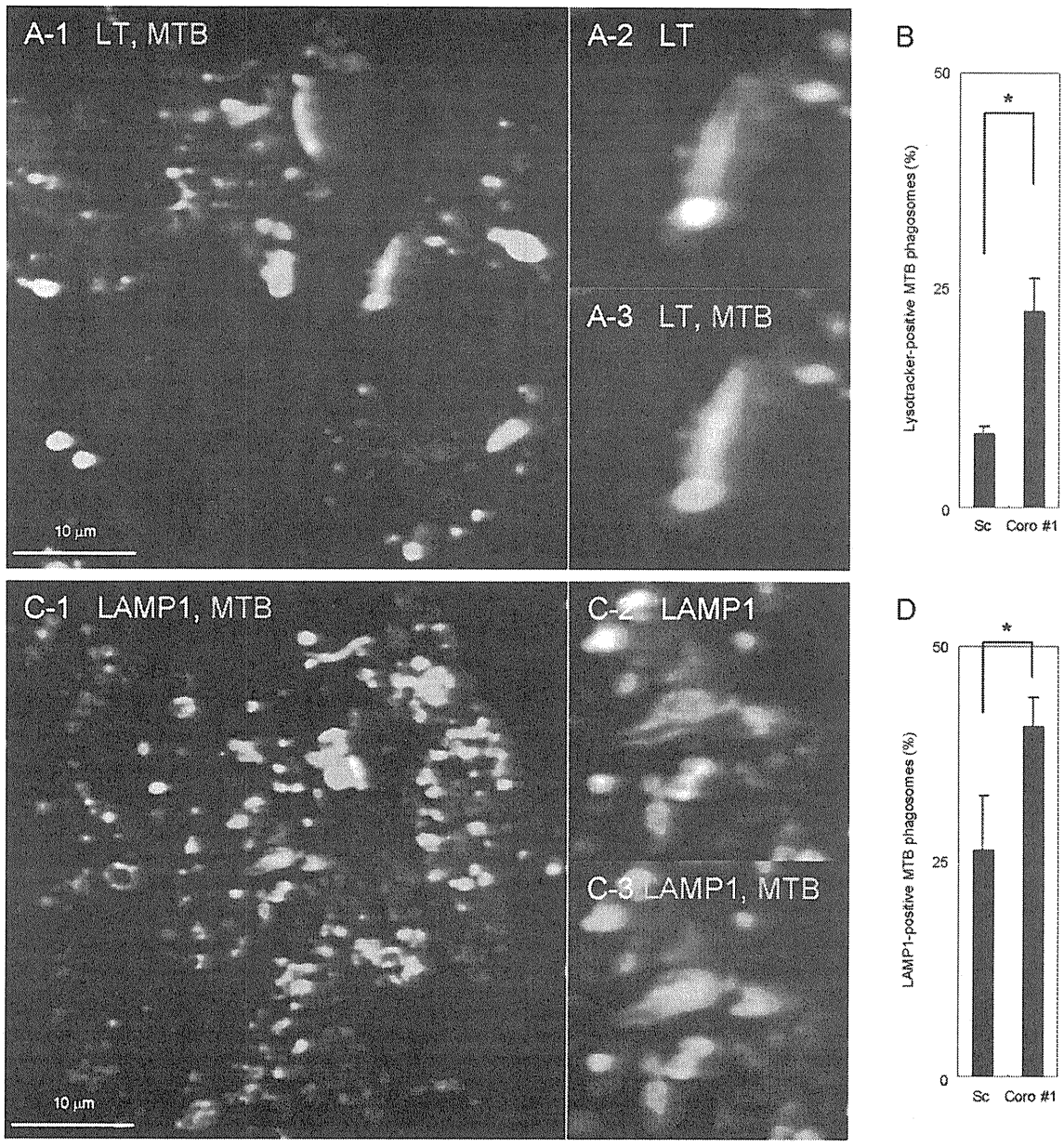

Fig. 2. Maturation of *M. tuberculosis*-containing phagosomes in Coro1a KD macrophages.
A. Acidification of mycobacterial phagosomes in Coro1a KD macrophages. Macrophages transfected with Coro1a-specific siRNA were infected with DsRed-expressing *M. tuberculosis* for 24 h and stained with LysoTracker. Infected macrophages were fixed and observed by laser scanning confocal microscopy (LSCM). Enlarged images of A-1 are represented in A-2 and A-3.
B. The proportion of *M. tuberculosis*-containing phagosomes labelled with LysoTracker in Coro1a KD macrophages. The numbers of LysoTracker-positive *M. tuberculosis*-containing phagosomes in macrophages transfected with Coro1a-specific or scrambled siRNA were counted.
C. LAMP1 localization to mycobacterial phagosomes in Coro1a KD macrophages. Macrophages transfected with Coro1a-specific siRNA were infected with DsRed-expressing *M. tuberculosis* for 24 h. Infected macrophages were stained with anti-LAMP1 antibody and observed by LSCM. Enlarged images of C-1 are represented in C-2 and C-2.
D. The proportion of *M. tuberculosis*-containing phagosomes labelled with anti-LAMP1 antibody in Coro1a KD macrophages. The numbers of LAMP1-positive *M. tuberculosis*-containing phagosomes in macrophages transfected with Coro1a-specific or scrambled siRNA were counted. Data represent the means and the standard deviations (SD) of three independent experiments in which more than 200 phagosomes were counted for each condition. $*P < 0.05$ (unpaired Student's *t*-test); Sc, scrambled; Coro, Coro1a; MTB, *M. tuberculosis*; LT, LysoTracker.

inhibitor (Seglen and Gordon, 1982), and then infected with *M. tuberculosis*. The survival of *M. tuberculosis* in Coro1a KD macrophages was partially restored by treatment with 3-MA (Fig. 3A), suggesting that autophagic processes were involved in the inhibition of mycobacterial survival in Coro1a KD macrophages.

To further analyse the inhibitory mechanism of *M. tuberculosis* survival, we infected macrophages co-transfected with siRNAs for Coro1a and autophagy-related genes with *M. tuberculosis*. Atg3, Atg5 and Beclin1 are well-known autophagy-related proteins that drive the autophagy process (Mizushima and Levine, 2010). The targeting efficiencies of Coro1a and autophagy-related genes in Raw264.7 macrophages were confirmed by immunoblot analysis (Fig. 3E). Silencing of these autophagy-related proteins restored this inhibitory effect on *M. tuberculosis* survival in Coro1a KD macrophages (Fig. 3B–D). These results suggest that the induction of autophagy is involved in the promotion of *M. tuberculosis* eradication in Coro1a KD macrophages.

Autophagosome formation around M. tuberculosis*-containing phagosomes in Coro1a KD macrophages*

To confirm autophagosome formation in Coro1a KD macrophages infected with *M. tuberculosis*, we examined the localization of LC3, an autophagosome marker (Kabeya *et al.*, 2000), by fluorescence microscopy. Coro1a KD or control Raw264.7 macrophages were infected with DsRed-expressing *M. tuberculosis* and stained with anti-LC3 antibody. Only a small population of *M. tuberculosis*-containing phagosomes was LC3-positive in the control macrophages at 6 h post infection (p.i.) (Fig. 4A), supporting previous findings (Gutierrez *et al.*, 2004). LC3 recruitment to the mycobacterial phagosomes was further observed in Coro1a KD macrophages (Fig. 4B). Quantitative analysis revealed that the proportion of LC3-positive mycobacterial phagosomes was $> 30\%$ and $< 10\%$ in Coro1a KD and control macrophages respectively (Fig. 4E). Similar experiments employing LC3 fused with enhanced green fluorescence protein (EGFP-LC3) were also conducted. Raw264.7 macrophage stably expressing EGFP-LC3 were infected with DsRed-expressing *M. tuberculosis* for 2, 6 or 24 h. LC3 again localized to a small population of mycobacterial phagosome in control macrophages (Fig. 4C), while the number of LC3-positive mycobacterial phagosomes increased in Coro1a KD macrophages at 6 h p.i. (Fig. 4D). Quantitative analysis revealed that the proportion of LC3-positive mycobacterial phagosomes in Coro1a KD macrophages was greater than 30% and 20% at 6 h and 24 h p.i., respectively, while such an increase was not observed in control macrophages (Fig. 4F).

The ultrastructure of *M. tuberculosis*-containing phagosomes in Coro1a KD macrophages was also observed by thin-section electron microscopy. In control macrophages, bacilli resided in single-membrane phagosomes (Fig. 5A). In contrast, bacilli were surrounded by multiple membrane structures that were characteristic of autophagic vacuoles (Eskelinen, 2005) in Coro1a KD macrophages (Fig. 5B). We also found mycobacterial phagosomes with internal membranes in Coro1a KD macrophages (Fig. 5C) as previously reported (Gutierrez *et al.*, 2004). Quantitative analysis revealed that the proportion of bacilli associated with autophagic membrane structures reached more than 30% in Coro1a KD macrophages while that in control macrophages was less than 10% at 6 h p.i. (Fig. 5D). Collectively, these fluorescence and electron microscopy results suggest that autophagosome formation is induced around *M. tuberculosis*-containing phagosomes in Coro1a KD macrophages.

Validation of LC3 recruitment to M. tuberculosis*-containing phagosomes in Coro1a KD macrophages*

The recruitment of LC3 to *M. tuberculosis*-containing phagosomes was subsequently investigated in Coro1a KD macrophages treated with 3-MA (Fig. 6A) or simultaneously transfected with siRNA duplexes for autophagy-related genes (Fig. 6B). Both treatments abrogated the induction of LC3 recruitment to mycobacterial phagosomes in Coro1a KD macrophages.

Upon autophagy induction, LC3 is processed from a cytosolic form (LC3-I) to a membrane bound form (LC3-II) (Kabeya *et al.*, 2000). We first attempted to confirm the autophagy induction by immunoblot analysis using whole-cell lysates, but no significant increase in LC3 processing was observed in Coro1a KD and control macrophages infected with *M. tuberculosis* (Fig. 7A and D). We also found that no significant changes of LC3 processing in control or Coro1a KD macrophages infected with *M. tuberculosis* at the different infection rates (Fig. S1). The treatment with NH_4Cl or bafilomycin A1 achieved the similar accumulation of LC3-II in both control and Coro1a KD macrophages infected with *M. tuberculosis* (Fig. 7B and E), suggesting the normal autophagic flux in these macrophages. We next examined the recruitment of LC3 using isolated *M. tuberculosis*-containing phagosomes in Coro1a KD macrophages by immunoblot analysis (Fig. 7C). Enrichment of LC3-II was observed in the phagosomal fraction from Coro1a KD macrophages when compared with that from the control macrophages. Densitometric analysis revealed that the amount of LC3-II in the phagosomal fraction from Coro1a KD macrophages increased to approximately 2.7 times that observed for the control macrophages (Fig. 7F). This biochemical analysis

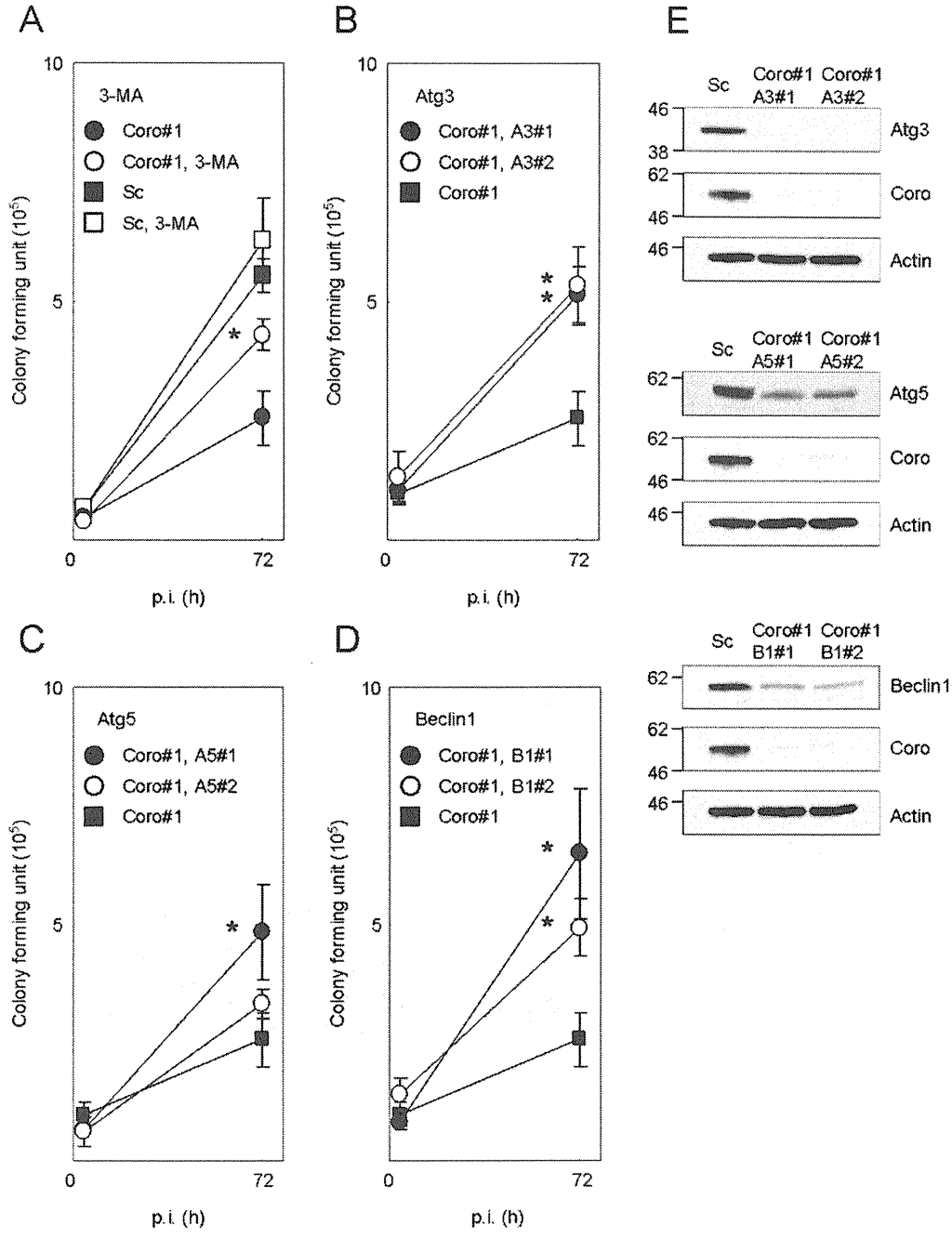

Fig. 3. Treatment with 3-MA or siRNA for autophagy-related genes suppressed the inhibition of *M. tuberculosis* proliferation in Coro1a KD macrophages.

A. Proliferation of *M. tuberculosis* in Coro1a KD macrophages treated with 3-MA. Macrophages transfected with Coro1a-specific or scrambled siRNA were treated with or without 3-MA (10 mM) for 1 h and then infected with *M. tuberculosis*. Viable mycobacteria number was determined by cfu assay at 4 h and 72 h p.i. The data represent the means and SEM of three independent experiments. The numbers of cfu at 72 p.i. in Coro1a KD macrophages treated with or without 3-MA were compared. $*P < 0.05$ (unpaired Student's *t*-test).

B–D. Proliferation of *M. tuberculosis* in macrophages transfected with siRNA for Coro1a and autophagy-related genes. Macrophages were transfected with siRNAs for Coro1a and Atg3 (B), Coro1a and Atg5 (C) or Coro1a and Beclin1 (D). Transfected macrophages were then infected with *M. tuberculosis*. Colony-forming unit assay was performed at 4 h and 72 h p.i. The data represent the means and SEM of three independent experiments. The numbers of cfu at 72 h p.i. in Coro1a KD macrophages transfected with or without siRNA for autophagy-related genes were compared. $*P < 0.05$ (unpaired Student's *t*-test).

E. Immunoblot analysis on the silencing effects of Coro1a and autophagy-related genes. Macrophages were transfected with siRNA for Coro1a and the indicated autophagy-related genes for 48 h. Whole-cell lysates were subjected to SDS-PAGE, followed by immunoblot analysis using the indicated antibodies.

Sc, scrambled; Coro, Coro1a; A3, Atg3; A5, Atg5; B1, Beclin1.

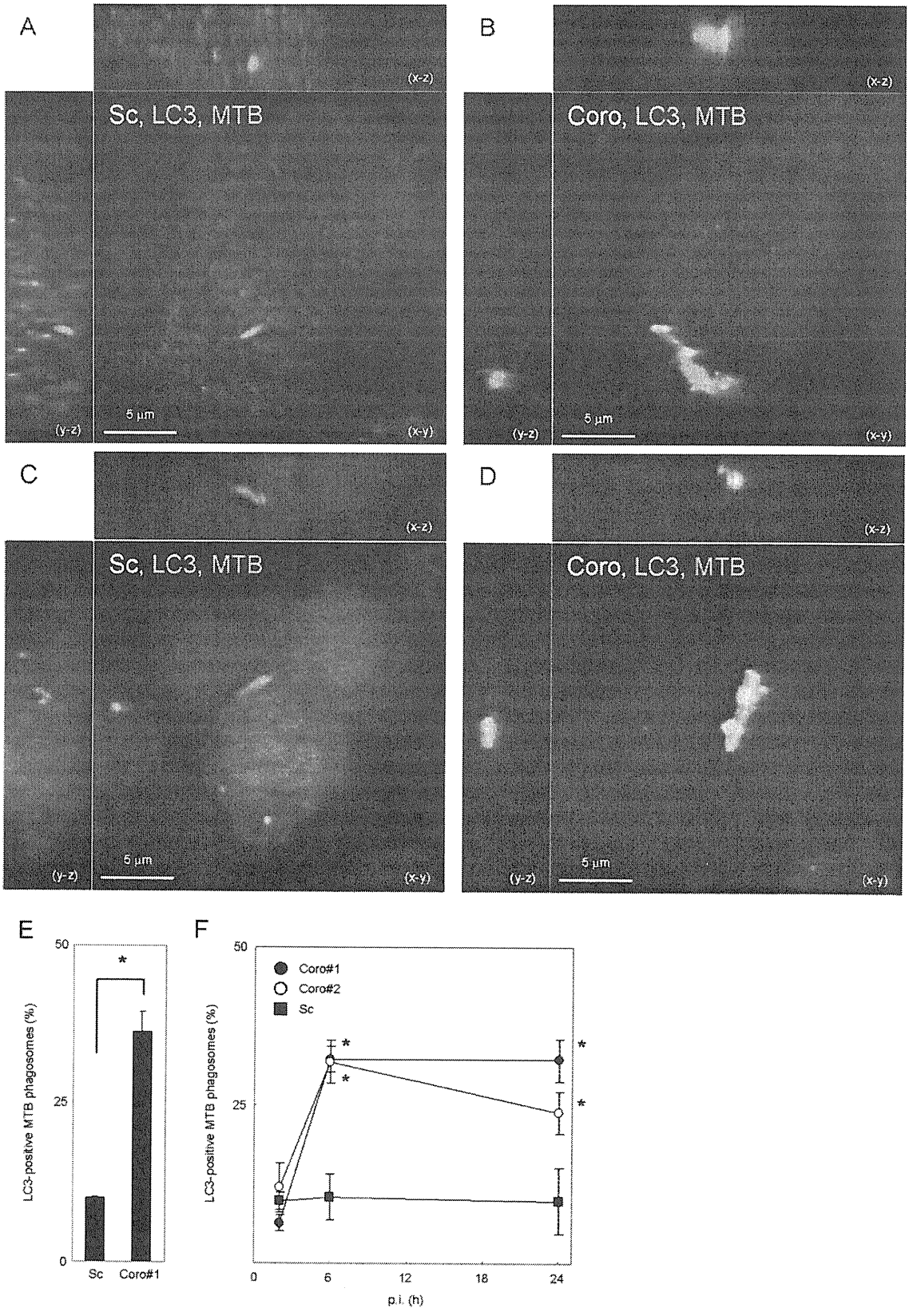

Fig. 4. LC3 recruitment to mycobacterial phagosomes in Coro1a KD macrophages.
A and B. LC3 recruitment to *M. tuberculosis*-containing phagosomes in Coro1a KD macrophages by immunofluorescence microscopy. Macrophages transfected with scrambled (A) or Coro1a-specific (B) siRNA were infected with DsRed-expressing *M. tuberculosis* for 6 h. Infected macrophages were fixed and stained with anti-LC3 antibody, and then observed with LSCM. Projections of focal planes with y–z and x–z side views are represented.
C and D. Recruitment of LC3 fused with EGFP (EGFP-LC3) to *M. tuberculosis*-containing phagosomes in Coro1a KD macrophages. Macrophages stably expressing EGFP-LC3 were transfected with scrambled (C) or Coro1a-specific (D) siRNA and infected with DsRed-expressing *M. tuberculosis* for 6 h. Infected macrophages were fixed and observed by LSCM. Projections of focal planes with y–z and x–z side views are represented.
E. The proportion of *M. tuberculosis*-containing phagosomes labelled with anti-LC3 antibody in Coro1a KD macrophages. Macrophages transfected with Coro1a-specific or scrambled siRNA were infected with DsRed-expressing *M. tuberculosis* for 6 h. Cells were then stained with anti-LC3 antibody and observed with LSCM. The number of LC3-positive *M. tuberculosis*-containing phagosomes was counted.
F. The proportion of *M. tuberculosis*-containing phagosomes labelled with EGFP-LC3. Macrophages stably expressing EGFP-LC3 were transfected with Coro1a or scrambled siRNA and infected with DsRed-expressing *M. tuberculosis* for 2, 6 and 24 h. Cells were fixed and observed with LSCM. The numbers of LC3-positive mycobacterial phagosomes were counted.
Data represent the mean and SD of three independent experiments in which more than 200 phagosomes were counted for each condition. $^*P < 0.05$ (unpaired Student's *t*-test). Sc, scrambled; Coro, Coro1a; MTB, *M. tuberculosis*.

further supports that the recruitment of LC3 to *M. tuberculosis*-containing phagosomes is facilitated by Coro1a depletion in macrophages.

Localization of p62, ubiquitin and LAMP1 to LC3-positive mycobacterial phagosomes in Coro1a KD macrophages

To characterize the LC3-positive mycobacterial phagosomes in Coro1a KD macrophages, we examined the localization of p62/SQSTM1 (p62), ubiquitin and LAMP1 to LC3-positive mycobacterial phagosomes (Fig. 8). Bacteria in cytosols are targeted by the ubiquitin system (Perrin *et al.*, 2004) and the autophagic degradation (Dupont *et al.*, 2009). p62 is involved in targeting intracellular bacteria to the autophagy pathway (Dupont *et al.*, 2009; Zheng *et al.*, 2009) and indispensable for autophagic elimination of mycobacteria in macrophages (Ponpuak *et al.*, 2011). We found that p62 and ubiquitin localized to LC3-positive mycobacterial phagosomes in Coro1a KD macrophages (Fig. 8A and C). The proportion of LC3-positive mycobacterial phagosomes colocalized with p62 and/or ubiquitin increased up to 24 h p.i. (Fig. 8B and D). In addition, the proportion of LC3-positive mycobacterial phagosomes colocalized with LAMP1 also increased up to 24 h p.i. (Fig. 8E and F). These results indicate that p62, ubiquitin and/or LAMP1 are recruited to LC3-positive mycobacterial phagosomes in Coro1a KD macrophages during infection.

Phosphorylation of p38 MAPK is induced by M. tuberculosis *infection in Coro1a KD macrophages*

As mitogen-activated protein kinase (MAPK) signalling pathways are involved in autophagy induction (Esclatine *et al.*, 2009), we next examined which MAPK signalling pathways were affected by *M. tuberculosis* infection in Coro1a KD macrophages (Fig. 9). Macrophages transfected with Coro1a-specific or scrambled siRNA were infected with *M. tuberculosis*, and phosphorylation of ERK1/2, p38 and JNK was investigated by immunoblot analysis. No significant difference in ERK1/2 activation kinetics was detected between control and Coro1a KD macrophages after *M. tuberculosis* infection. JNK activation was not detected in both control and Coro1a KD macrophages (data not shown). In contrast, a significant increase in p38 phosphorylation was observed in Coro1a KD macrophages, while no induction was detected in control macrophages (Fig. 9A).

The recruitment of LC3 to *M. tuberculosis*-containing phagosomes in Coro1a KD macrophages treated with various inhibitors for MAPK signalling pathways was also investigated by imaging analysis. Inhibition of p38 signalling, but not MEK1 or JNK signalling, reduced the proportion of LC3-positive mycobacterial phagosomes in Coro1a KD macrophages (Fig. 9B), further supporting that the p38 MAPK pathway is a target of Coro1a in the inhibition of autophagosome formation around *M. tuberculosis*-containing phagosomes.

Induction of LC3 recruitment to M. tuberculosis*-containing phagosomes in Coro1a KD alveolar macrophages and bone marrow-derived macrophages*

Mycobacterium tuberculosis is inhaled via aerosols into the lung, where alveolar macrophages (AM) are the first line of defence (Russell, 2001; 2007). We investigated whether autophagosome formation around *M. tuberculosis*-containing phagosomes is also induced in AM by Coro1a depletion. MH-S is an AM cell line, in which *M. tuberculosis* can survive and proliferate (Mbawuike and Herscowitz, 1989; Sirakova *et al.*, 2003). MH-S macrophages were transfected with Coro1a siRNA (Fig. 10A) and infected with *M. tuberculosis*. When AM were transfected with scrambled siRNA, LC3 did not localize to mycobacterial phagosomes (data not shown). In contrast, the recruitment of LC3 to mycobacterial phagosomes